Sequential Extraction of Organosolv Lignin from Chinese Quince Fruit: Structural Features and Antioxidant Activities of the Obtained Fractions

Xi-Chuang Cheng, Zhao Qin,* Qiao-Li Yang, Hua-Min Liu,* Xue-De Wang, and Yu-Lan Liu

Lignin from the Chinese quince (*Chaenomeles sinensis*) fruit offers a promising source of natural antioxidant for industrial applications. However, the utilization of Chinese quince fruit lignin is restricted by its inhomogeneous nature. Accordingly, Chinese quince fruit lignin was sequentially fractionated with organic solvents of increasing dissolving capacity to prepare homogeneous lignin fractions. The GPC (gel permeation chromatography) results showed that the molecular weights of lignin fractions increased from dichloromethane fraction to dioxane/water fraction. The five lignin fractions were also compared with respect to yield, carbohydrate content, thermal stability, inter-unit linkages, S/G ratios, and phenolic OH content. Among the five fractions, the ethyl acetate fraction showed a lower proportion of *β*-O-4' linkages (48.4%), the highest thermal stability, the highest phenolic OH content (2.8 mmol/g), and the highest DPPH (1,1-diphenyl-2-picrylhydrazyl) radical scavenging index and reducing power. The high antioxidant performance of the ethyl acetate fraction implies that it can be used as a natural antioxidant. This study shows that sequential solvent fractionation of lignin can produce homogeneous fractions with enhanced antioxidant performance. In addition, it demonstrates that Chinese quince fruits are a potentially valuable natural resource.

Keywords: Chinese quince fruits; Lignin fractionation; Characterization; Antioxidant property

Contact information: College of Food Science and Technology, Henan University of Technology, Zhengzhou 450001 Henan, China;
** Corresponding authors: qinzhao505@163.com; liuhuamin5108@163.com*

INTRODUCTION

Lignin is the most abundant natural phenolic compound (Crestini *et al.* 2011). As a polyphenolic macromolecule, lignin shows antioxidant properties, and its prospective use as a natural antioxidant has been considered by many studies (Dizhbite *et al.* 2004; Pan *et al.* 2006; Michelin *et al.* 2018). Lignin's antioxidant properties are attributed to its structure, in that each molecule contains hydroxyl groups linked to benzene rings; these hydroxyl groups can readily capture and neutralize free radicals (Kim *et al.* 2019). Despite strong antioxidant properties of lignin, its application has been limited. Catignani and Carter (1982) researched the antioxidant properties of lignins and found that lignin had a positive effect on delaying the oxidation of tocopherol-stripped corn oil. Through evaluating the effects of industrial lignins from different lignocellulosic materials on two immortalized cell lines, Ugartondo *et al.* (2008) found that lignin is safe to the human keratinocyte cell line and suggested that lignin could be used as a potential antioxidant in pharmaceuticals and cosmetics. Vinardell *et al.* (2008) illustrated that lignins exhibited

high antioxidant performance and were safe for the eyes and skin, and they proposed the potential use of lignin in pharmaceuticals.

However, lignins are characterized by high polydispersity of molecular weight (M_w) and complexity of chemical groups that inevitably influence their antioxidant properties. Simply, their properties can hinder their industrial utilization. Several approaches have been proposed to homogenize the lignin molecule, such as GPC, membrane-assisted ultrafiltration, selective precipitation based on pH, organic solvent fractionation, *etc.* (Kirk *et al.* 1969; Li *et al.* 2012; Santos *et al.* 2014; An *et al.* 2017; Costa *et al.* 2018; Song *et al.* 2020). Compared with other methodologies, sequential solvent fractionation is a more simple, eco-friendly, and cost-effective method to improve the antioxidant properties of lignin samples (Li *et al.* 2012; Arshanitsa *et al.* 2013). Sequential solvent fractionation is a process that yields different fractions based on the different solubility of specific lignin fragments in the selected solvent with different polarities. Some of these different fractions have lower molecular weights and more numerous functional groups, often with improved antioxidant properties (Arshanitsa *et al.* 2013; Lange *et al.* 2016).

Chinese quince (*Chaenomeles sinen*sis) (Rosaceae) is widely found in China. Its fruits have been used as a Chinese herbal medicine for treating coughs and throat diseases. However, the raw fruits cannot be eaten directly because of their strong acidity and astringency (Hamauzu *et al.* 2010). The abundant lignin in the fruits makes their flesh woody, hard, and astringent. However, the lignin from Chinese quince fruit offers a promising source of natural antioxidant for industrial applications. Unfortunately, when compared with other lignocellulosic materials, such as hard-woods, soft-woods, and grasses, knowledge of lignin from Chinese quince fruit is still limited, especially the knowledge demanded for the industrial application of lignin from quince fruit.

The organosolv process has been demonstrated as an effective technique for the collection of sulfur-free, low molecular-weight lignin with few inorganic impurities (Hamauzu *et al.* 2010; Huang *et al.* 2020). In a previous study, the effect of extraction conditions on auto-catalyzed ethanol organosolv lignin (AEOL) from Chinese quince fruit was assessed, confirming the optimal conditions to collect AEOL with high antioxidant performance (Cheng *et al.* 2020). However, the antioxidant performance of AEOL was restricted by its high polydispersity of molecular weight (M_w) and diverse chemical group composition. In the present study, AEOL was fractionated into five fractions using a sequential solvent fractionation process. The monosaccharide composition, molecular weight distribution, S/G ratios, phenolic OH content, thermostability, and antioxidant properties of AEOL and its five sub-fractions were investigated.

EXPERIMENTAL

Materials and Methods

Mature fruits from Chinese quince plants were acquired from an open market in Kaifeng, China. The fruits were cut into 3 mm to 5 mm slices and then freeze-dried. The dried samples were pulverized to pass through a 40-mesh sieve. The wax and other impurities from the sieved sample were removed in a Soxhlet extraction apparatus using toluene/ethanol (2:1, v/v) before use. However, there is probably a small amount of lower-mass phenolic compounds after the Soxhlet extraction step. The AEOL was isolated according to a previous publication (Cheng *et al.* 2020). The chemical composition of

AEOL was lignin 95.02% ± 1.05%, glucosan 0.21%, xylan 2.71%, arabinan 0.20%, and galactan 0.26%. All chemical reagents were analytical grade.

Solvent fractionation of AEOL

Auto-catalyzed ethanol organosolv lignin was sequentially fractionated by five organic solvents, namely dichloromethane, ethyl acetate, methanol, acetone, and dioxane/water (9/1, v/v). Auto-catalyzed ethanol organosolv lignin (10 g) was put into an Erlenmeyer flask containing 400 mL of dichloromethane. After stirring for 120 min, the mixture was filtered, and the undissolved material was resuspended for a second identical extraction. Next, the filtrates from both steps were combined and rotary evaporated. The insoluble material was extracted by the next solvent. After being freeze-dried, the dichloromethane fraction (F1) was obtained. Then, the ethyl acetate fraction (F2), methanol fraction (F3), acetone fraction (F4), and dioxane/water fraction (F5) were prepared. The yields of the five lignin fractions were expressed in % of dry original lignin (AEOL).

Lignin characterization

The carbohydrate moiety of lignin fractions was determined with a high-performance anion-exchange chromatography (HPAEC) system (ICS-3000; Dionex, Sunnyvale, CA, USA), as reported by Li *et al.* (2012). Lignin samples (5 mg) were treated with 125 μL of 72% H_2SO_4 for 45 min at room temperature. After diluting H_2SO_4 to 4%, the lignin fractions were continuously hydrolyzed for 3 h at 105 °C. Fourier-transform infrared spectroscopy (FT-IR) spectra of lignin fractions were recorded using a Vector 22 spectrometer (Bruker, Billerica, MA, USA). Lignins (1 to 2 mg) were ground with dried KBr and further compacted into thin pellets. Spectra were acquired in the range 4,000 to 400 cm^{-1} with 32 scans and a 4 cm^{-1} resolution. The thermostability of lignin fractions was analyzed using a thermogravimetric system (DTG-60; Shimadzu, Kyoto, Japan). Samples (10 mg) were heated from 40 °C to 700 °C at a rate of 10 °C/min in a nitrogen atmosphere. The molecular weight distributions of the acetylated lignin fractions were determined by GPC (Waters 1525; Waters, Milford, MA, USA). Acetylation of lignin fractions was carried out as reported previously (Cheng *et al.* 2020). Polystyrene standards with different molecular weights (M_w in the range of 500 to 1,000,000) were used to calibrate the GPC system. Pyrolysis-gas chromatography-mass spectrometry (Py-GC/MS) analyses of AEOL and its five lignin fractions were performed using a 2020 microfurnace pyrolyzer (Frontier Laboratories, Koriyama, Japan) connected to a GC/MS (Agilent 6890; Agilent Technologies, Santa Clara, CA, USA). Pyrolysis was performed at 500 °C for 20 s. The GC oven temperature program was as follows: 50 °C (hold 4 min) → 100 °C (rate 20 °C/min) → 280 °C (rate 6 °C/min) (hold for 5 min). Quantitative 2D heteronuclear single quantum coherence (HSQC) spectra were obtained using an AVANCE III 400 MHz spectrometer (Bruker, Billerica, MA, USA). The lignin fraction (50 mg) was dissolved in 500 μL DMSO-d_6. The spectra were recorded using the Bruker standard pulse program (hsqcetgpsi2; Billerica, MA, USA) (Wen *et al.* 2013). Quantitative ^{31}P nuclear magnetic resonance (NMR) spectra of lignin fractions were obtained according to a published procedure (Qin *et al.* 2018a).

Antioxidant performance

The DPPH (1,1-diphenyl-2-picrylhydrazyl) assay was performed based on the description of a published procedure (Qin *et al.* 2018a). Briefly, 150 μL of a lignin sample in 90% dioxane (with seven different concentrations from 0.05 to 1.0 mg/mL) was added

to 2.85 mL DPPH in methanol (0.024 mg/mL) and then kept in the dark for 20 min. The absorbance was recorded at 517 nm using a spectrometer. Each assay was done in triplicate. Butylated hydroxytoluene (BHT) was used as a reference. The scavenging activity was calculated using Eq. 1,

$$\text{Scavaging activity (\%)} = \left[\frac{(A_0 - A_1)}{A_0}\right] \times 100 \quad (1)$$

where A_0 is the absorbance of the blank sample solution, and A_1 is the absorbance of the lignin sample solution. IC_{50} is defined as the lignin concentration providing 50% radical scavenging. Radical scavenging index (RSI, the inverse of IC_{50}) was used to characterize the antioxidant performance of lignin fractions.

The reducing power of lignin fractions was studied according to the method of An *et al.* (2017) with some modifications. A 1 mL lignin sample in 90% dioxane (with concentrations ranging from 0.05 to 0.3 mg/mL) was mixed with 1 mL 0.2 M phosphate buffer (pH = 6.6) and 1 mL $K_3[Fe(CN)_6]$ solution (1%, w/w) and then warmed in a thermostatic pot at 50 °C for 20 min.

Subsequently, 1 mL trichloroacetic acid (10%, w/w) was added, and the solution was centrifuged at 4,000 rpm for 10 min. The reducing reaction was started by mixing 1.5 mL supernatant, 1.5 mL deionized water, and 0.3 mL $FeCl_3$ solution (0.1%, w/w) and then letting the mixture rest for 8 min. Absorbance of the mixture was recorded at 700 nm. Each assay was done in triplicate.

RESULTS AND DISCUSSION

Yield of Lignin Fractions

In this work, AEOL from Chinese quince fruits was sequentially fractionated using various organic solvents. The selection of organic solvents was determined according to their Hildebrand solubility parameters (δ) and capacities to form hydrogen bonds with lignin (Passoni *et al.* 2016). The capability of solvents to dissolve lignin increases as their δ value approaches to 11. Compared with higher molecular weight fractions, lower molecular weight fractions exhibited higher solubility in organic solvents with weak or moderate hydrogen bonding ability with a wide range of δ values (Li *et al.* 2012). In the present study, five solvents were applied based on their polarities, Hildebrand solubility parameters (ranging from 7.4 to 14.3), and capacity to form hydrogen bonds with lignin. The yield of extraction fractions is listed in Table 1.

The high yield of F3 (43.8%) may be due to abundant hydroxyl and carbonyl groups, which enhanced the ability of methanol to establish hydrogen bonding interactions with AEOL such that AEOL dissolved more readily in it (Passoni *et al.* 2016). Notably, all the lignin samples were free-flowing powders except for the dichloromethane-soluble fraction, which was a slightly sticky, dark brown solid. This was probably because the presence of extractives, such as fatty acids and resins in the dichloromethane-soluble fraction. A similar result was reported by Li *et al.* (2012), who sequentially fractionated bamboo organosolv lignin using organic solvents and found that the ether fraction of the starting lignin was a sticky residue. According to the literature, the existence of extractives (such as resinous materials) in the ether-soluble fraction was probably responsible for the formation of sticky residue.

Table 1. Yield, Molecular Weight, and Sugar Compositions of Lignin Fractions

Lignin Fractions [a]	Yield (%)	M_n (g/mol)	M_w (g/mol)	M_w/M_n	Total Sugar (%)	Monosaccharide [b] (Based on Total Sugar, %)					
						Glu	Xyl	Ara	Gal	Gal-A	Glu-A
AEOL	-	1193	3692	3.1	3.5	6.1	77.4	5.8	7.5	2.4	0.8
F1	11.3 ± 0.35	428	647	1.5	0.8	14.8	55.1	6.9	10.4	5.2	7.7
F2	13.5 ± 0.34	670	1082	1.6	2.7	37.3	52.6	2.5	3.7	3.4	0.6
F3	43.8 ± 1.03	1519	3342	2.2	1.9	7.4	67.3	8.0	7.7	6.5	3.1
F4	8.7 ± 0.26	4519	11298	2.5	1.3	35.1	38.0	6.2	10.3	8.6	1.8
F5	18.6 ± 0.67	5758	11603	2.0	6.4	5.0	84.6	1.9	6.9	1.3	0.2

[a] AEOL = auto-catalyzed ethanol organosolv lignin; F1 = dichloromethane fraction; F2 = ethyl acetate fraction; F3 = methanol fraction; F4 = acetone fraction; F5 = dioxane/water fraction
[b] Glu = glucose; Xyl = xylose; Ara = arabinose; Gal = galactose; Gal-A = galacturonic acid; Glu-A = glucuronic acid

Sugar Analysis

To analyze the carbohydrate moieties in AEOL and its five lignin fractions, a sugar analysis was performed. All the sugars referred to here were formed from the breakdown of the polysaccharides present in the AEOL. The total sugar content of AEOL was 3.5% (Table 1), indicating that the AEOL that separated from the Chinese quince fruit had relatively little carbohydrate. In addition, results revealed a difference between total sugar contents in the lignin fractions and in AEOL, which meant that the sugar composition of the lignin was influenced by the fractionation. For all the lignin samples, xylose represented the highest percentage of the total sugar, suggesting that xylans were the predominant carbohydrate in all the lignin fractions. Compared with unfractionated AEOL, the total sugar contents of separated lignin fractions were reduced except for the F5 fraction. The reduced sugar contents of the lignin fractions indicated that the sequential solvent fractionation process eliminated carbohydrates and increased the purity of the lignin. The high purity of lignins from Chinese quince fruits is beneficial for both structural elucidation and industrial application. Generally, the carbohydrate linked to lignin exist as lignin-carbohydrate complexes, and the components are formed by covalent linkages between carbohydrates and lignin (Qin *et al.* 2018b). Because of these covalent linkages, carbohydrates are hard to remove completely from lignin.

Molecular Weight Distributions

Figure 1 depicts the GPC chromatograms of five lignin fractions and AEOL. The AEOL exhibited a broad molecular weight distribution, and all five fractions presented narrower molecular weight distributions. The F1, F2, and F3 fractions showed higher molecular weight distributions with a noticeable contribution given by low-molecular-weight lignins ($M_w < 5000$), whereas F4 and F5 fractions showed higher molecular weights. The molecular weight distributions can provide insights for quantitative comparison of lignin fractions. The M_w and M_n of AEOL were 3692 g/mol and 1193 g/mol, respectively, and its polydispersity was 3.1 (Table 1). After fractionation, the polydispersity of obtained lignin fractions decreased, with F1 and F2 showing a polydispersity of 1.5 and 1.6,

respectively. The M_w of the lignin fractions increased from 647 g/mol (F1) to 11603 g/mol (F5); equally, the M_n increased from 428 g/mol (F1) to 5758 g/mol (F5). The increased molecular weight suggested that lower molecular weight lignin had higher solubility in organic solvents compared with higher molecular weight lignin. Overall, the GPC results indicated that sequential organic solvent extraction was a reliable technique to subdivide AEOL into fractions with a low molecular weight and narrow polydispersity.

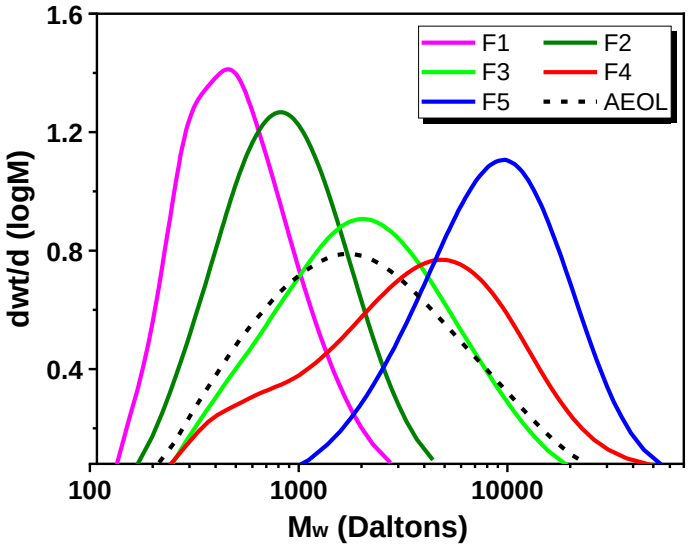

Fig. 1. Molecular weight distributions of AEOL and five lignin fractions

FT-IR Analysis

The structural features of each resulting lignin fraction were studied by FT-IR spectrometry (Fig. 2).

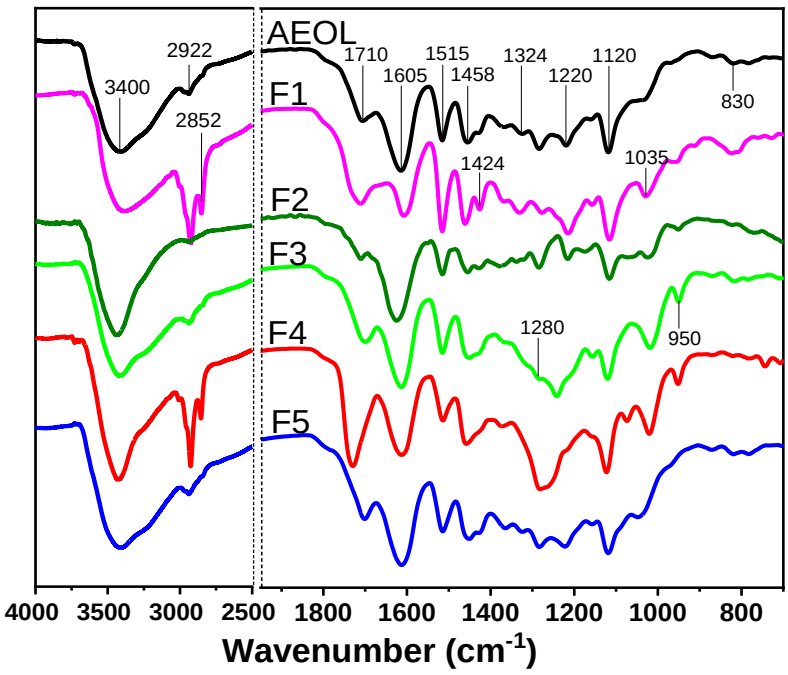

Fig. 2. FT-IR spectra of AEOL and five lignin fractions

The variable intensities of the bands for phenolic and aliphatic OH groups, assigned at 3400 cm^{-1}, were highest in F2, indicating a higher concentration of OH groups in the ethyl acetate-soluble fraction. In contrast, the variable intensity of the same band was lowest in F1. The absorptions at 1605, 1515, and 1424 cm^{-1} were attributed to aromatic skeleton vibration, revealing that the "core" of lignin fractions was not broken during sequential solvent fractionation (Qin *et al.* 2018a).

Bands for the C-H asymmetric deformations were observed at 1458 cm^{-1}. A remarkable reduction in intensity was recorded at 1280 cm^{-1} of F3 compared to AEOL, which is related to G units (Qin *et al.* 2018a). The bands at 1324, 1220, and 1120 cm^{-1} correspond to S units (Inkrod *et al.* 2018). The signals at 1035 cm^{-1} were attributed to aromatic C-H in-plane deformation vibrations, whereas the signals at 830 cm^{-1} were assigned to C-H out-of-plane stretching (Passoni *et al.* 2016). In addition, the absorption of the C-H stretching of aliphatic groups showed strong intensity peaks for F1 and F4 at 2922 cm^{-1} and 2852 cm^{-1}, respectively, which could mean the presence of aliphatic groups at higher concentrations in F1 and F4 fractions (Smink *et al.* 2020). Similarly, the stronger peak intensities at 1710 cm^{-1} in the spectra of F1 and F4 fractions indicated a relative higher content of conjugated carbonyl groups (Inkrod *et al.* 2018). Consequently, F1 and F4 fractions likely showed lower antioxidant activity because of the negative effect of aliphatic groups and conjugated carbonyl groups on the lignin antioxidant performance (Dizhbite *et al.* 2004; Pan *et al.* 2006).

Py-GC/MS Analysis

Pyrolysis-gas chromatography-mass spectrometry is a useful technique to characterize the constituents of lignin fractions. The programs of AEOL and five fractions are depicted in supplementary information. As shown in Table 2, the pyrolysis products derived from *p*-hydroxyphenyl (H), guaiacyl (G), and syringyl (S) phenols were clearly identified. The five lignin fractions released pyrolysis products similar to AEOL during the pyrolysis process, indicating that the sequential extraction was non-destructive to the original lignin.

The S/G ratios of AEOL and the five lignin fractions are also shown in Table 2. It should be noted that 2-methoxy-4-vinyl-phenol (peak 13) was not used to calculate the S/G ratios because a major part of 2-methoxy-4-vinyl-phenol does not originate from lignin but from *p*-hydroxycinnamates, such as ferulates on arabinoxylans that are not associated with the core lignin structural units (del Río *et al.* 2012; Qin *et al.* 2018c). The S/G ratios of AEOL, F1, F4, and F5 were higher than 1.0, suggesting that the AEOL of Chinese quince fruit and its dichloromethane, acetone, and dioxane fractions were S-rich lignin. In contrast, the ethyl acetate and methanol fractions were G-rich lignin. In general, the S/G ratios obtained by Py-GC/MS showed a trend consistent with, but lower than, that obtained by the 2D-HSQC NMR method. Demethoxylation during pyrolysis may explain these differences.

More G-type degradation products could be produced during pyrolysis because the demethoxylation of S-units occurred more easily than that of G-units, thus the S/G ratio decreased (Wen *et al.* 2015). Overall, the results of Py-GC/MS analysis demonstrated that lignin fractions with different amounts and types of side-chain groups could be obtained by sequential solvent extraction. Diversity in functional groups gives the lignin fractions versatility and selectivity in antioxidant preparation.

Table 2. Identification and Relative Abundance (%) of the Lignin-derived Compounds from the Py-GC/MS of AEOL and Five Lignin Fractions

Compound	Origin	AEOL	F1	F2	F3	F4	F5
Phenol	H	1.1	0.5	0.3	0.7	0.1	0.5
Phenol, 2-methoxy-	G	8.1	3.2	7.6	4.9	6.8	4.2
p-Cresol	H	1.0	0.0	0.3	0.4	0.0	0.6
Phenol, 2-methoxy-3-methyl-	G	0.5	1.6	1.1	0.0	0.0	0.0
Benzene, 1,4-dimethoxy-	S	0.0	0.0	0.0	0.7	0.0	0.0
Creosol	G	7.4	7.7	10.4	9.9	4.9	9.1
Phenol, 2-ethyl-4-methyl-	H	0.0	0.0	0.4	1.2	0.0	0.0
Benzene, 1,4-dimethoxy-2-methyl-	S	0.0	1.1	0.0	0.0	0.0	0.0
Phenol, 4-ethyl-2-methoxy-	G	4.6	3.5	5.5	0.0	6.2	0.0
Catechol	H	1.3	0.0	2.9	9.6	9.2	0.0
Phenol, 2-propoxy-	H	0.0	0.0	0.0	0.0	0.0	16.2
1,2-Benzenediol, 3-methoxy-	G	14.6	3.8	10.8	7.6	6.2	15.6
2-Methoxy-4-vinylphenol	G	12.9	9.5	13.1	13.4	8.3	12.6
Benzoic acid, 4-hydroxy-3-methoxy-	G	0.0	0.0	0.0	15.2	0.0	0.0
Phenol, 5-methoxy-2,3,4-trimethyl-	G	0.0	1.6	0.0	0.0	0.0	0.0
Phenol, 2,6-dimethoxy-	S	13.1	18.8	27.2	17.0	16.1	13.0
1,2-Benzenediol, 4-methyl-	H	6.1	0.0	3.6	0.0	0.9	0.0
1,2,4-Trimethoxybenzene	S	12.4	0.0	3.6	0.0	12.6	5.3
Phenol, 4-methoxy-3-(methoxymethyl)-	G	0.0	0.0	0.0	0.0	4.4	0.0
Benzene, 1,2,3-trimethoxy-5-methyl-	S	8.2	0.0	0.0	0.0	3.8	7.0
Benzene, 2-ethoxy-1,3-dimethoxy-	S	0.0	4.8	0.0	0.0	0.0	0.0
5-Tert-butylpyrogallol	H	0.0	11.8	0.0	0.0	0.0	0.0
Ethanone, 1-(2,6-dihydroxy-4-methoxyphenyl)-	G	0.0	0.0	10.3	9.9	0.0	0.0
3',5'-Dimethoxyacetophenone	S	0.0	0.0	0.0	0.0	12.1	0.0
4-Methyl-2,5-dimethoxybenzaldehyde	S	0.0	0.0	0.0	8.1	0.0	10.0
Phenol, 2,6-dimethoxy-4-(2-propenyl)-	S	1.3	1.2	0.0	0.0	1.4	0.0
Benzaldehyde, 3,4-dimethoxy-, methylmonoacetal	S	0.0	0.0	0.0	0.0	0.0	2.7
Phenol, 2,6-dimethoxy-4-(2-propenyl)-	S	6.8	2.8	0.0	0.0	1.0	0.0
(2,5-Dimethoxyphenyl) acetone	S	0.0	0.0	0.0	0.0	0.0	0.6
Benzaldehyde, 4-hydroxy-3,5-dimethoxy-	S	0.0	5.8	0.0	0.0	0.0	0.0
Phenol,2,6-dimethoxy-4-(1E)-1-propen-1-yl-	S	0.0	0.0	0.0	0.0	6.1	0.0
Phenol, 2,6-dimethoxy-4-(2-propenyl)-	S	0.0	16.5	2.4	0.8	0.0	0.0
2,5-Dimethoxyterephthalic acid	S	0.0	0.0	0.0	0.0	0.0	2.3
Ethanone, 1-(4-hydroxy-3,5-dimethoxyphenyl)-	S	0.6	5.1	0.6	0.8	0.0	0.5
3,5-Dimethoxy-4-hydroxyphenylacetic acid	S	0.0	0.7	0.0	0.0	0.0	0.0
H%		9.5	12.3	7.5	11.9	10.1	17.2
G%		48.1	30.9	58.7	60.8	36.8	41.4
S%		42.4	56.8	33.8	27.4	53.1	41.4
S/G		1.2	2.7	0.7	0.6	1.9	1.4

Thermal Stability

The thermostability of AEOL and its five fractions were investigated by thermogravimetric analysis (TG) and derivative thermogravimetric analysis (DTG) analysis. The decomposition of the samples occurred in wide temperature ranges (Fig. 3). This could be explained by the presence of abundant aromatic rings with various branches in lignin (Yang *et al.* 2020). The 10% weight loss of a given sample can be defined as T_d (decomposition temperature) (Jiang *et al.* 2016). The T_d of F1, F2, F3, and F4 were

recorded at 261, 264, 248, and 261 °C, respectively, which were lower than that of AEOL (284 °C). This indicated that the thermal degradation of these four fractions occurred more quickly as compared with AEOL. The F5 fraction exhibited the highest decomposition temperature of 50% weight loss, which is likely because this sample had the greatest number of *β*-O-4' linkages among all lignin fractions. In addition, the F2 fraction showed the largest maximum decomposition temperature (T_{DTGmax}) (379 °C), which exhibited the high thermal stability of the ethyl acetate-soluble fraction at high temperatures. The high thermal stability of F2 was speculated to result from the low number of *β*-O-4' linkages (Zhou *et al.* 2016). In comparison, F1 showed the lowest temperatures in both 50% weight loss and maximum decomposition, presumably because it had the lowest molecular weight and it had components, such as fatty acids and resins, which tend to evaporate and/or degrade at relatively low temperatures (Song *et al.* 2020).

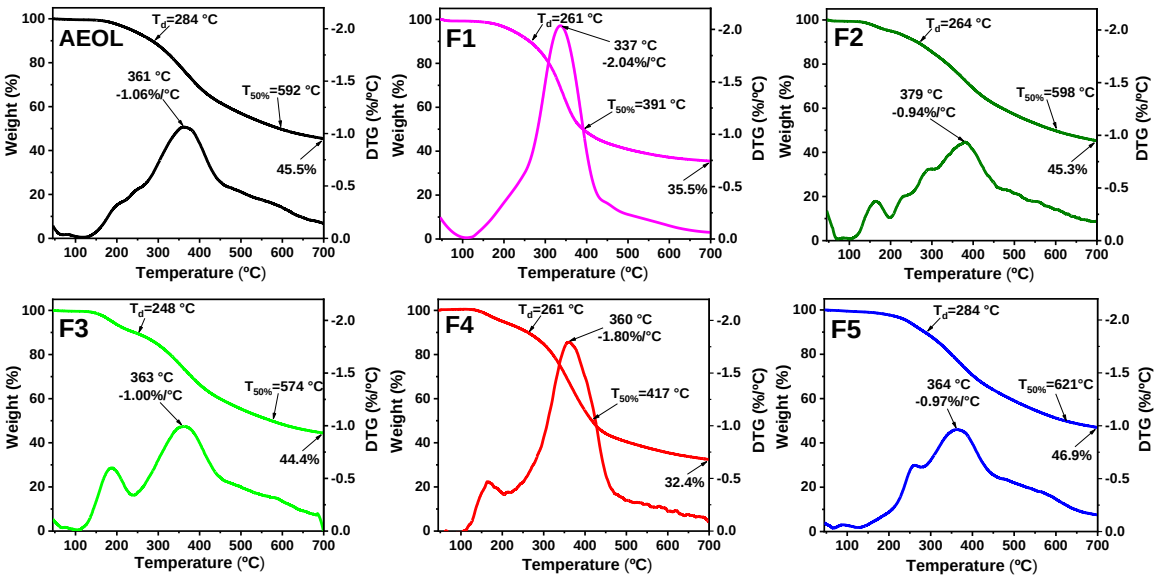

Fig. 3. The TG and DTG curves of lignin fractions; Decomposition temperatures at 10% weight loss, 50% weight loss, the char residues, the maximum decomposition rates, and the corresponding maximum decomposition temperatures are displayed.

The char residues at 700 °C of F2, F3, and F5 were 45.3%, 44.4%, and 46.9%, respectively, whereas that of the original lignin was 45.5%. The F1 and F4 fractions produced the lower char residues of 35.5% and 32.4%, respectively, which was presumably due to the high content of S-units in these two fractions, as revealed by their higher S/G ratios as indicated by the quantitative Py-GC/MS data (Table 2). Higher content of S-units, *i.e.*, methoxy groups (-OCH_3), in the lignin contributed to the low ratio of char residues of lignin (Cheng *et al.* 2020). Thus, the amount of char residues was inversely proportional to the S/G ratio of the lignin sample.

2D-HSQC NMR Spectra

An analysis using 2D-HSQC NMR was performed to obtain important structural information relevant to evaluating the effects of solvent fractionation on the various lignins. The HSQC spectra of AEOL, F2, and F4 are shown in Fig. 4, and the spectra were assigned according to previous reports (del Río *et al.* 2012; Qin *et al.* 2018c; Cheng *et al.* 2020). Six substructures were identified (Fig. 5), including *β*-O-4' aryl ethers (A, A'), resinol (B),

phenylcoumaran (C), spirodienone (D), and cinnamyl alcohol end-groups (I). Methoxyl groups were characterized by signals at δ_C/δ_H 56.3/3.75 ppm. The correlations corresponding of *β*-O-4' aryl ethers substructures were found with the signals at δ_C/δ_H 72.5/4.88 (A_α), 83.9/4.33 (A_β(G)), 86.6/4.13 (A_β(S)), and 60.2/3.34 to 3.73 ppm (A_γ). The α-ethoxylated *β*-O-4' aryl ethers substructures (A'_α) were founded by the correlations at δ_C/δ_H 81.0/4.60 ppm, implying the occurrence of α-ethoxylation during the pretreatment. Additionally, the methylene in α-ethoxylated *β*-O-4' aryl ethers substructures (A'_α-CH_2CH_3) was founded at δ_C/δ_H 65.3/3.38 ppm, which confirmed that α-ethoxylation had occurred in *β*-O-4' linkages (Huang *et al.* 2020).

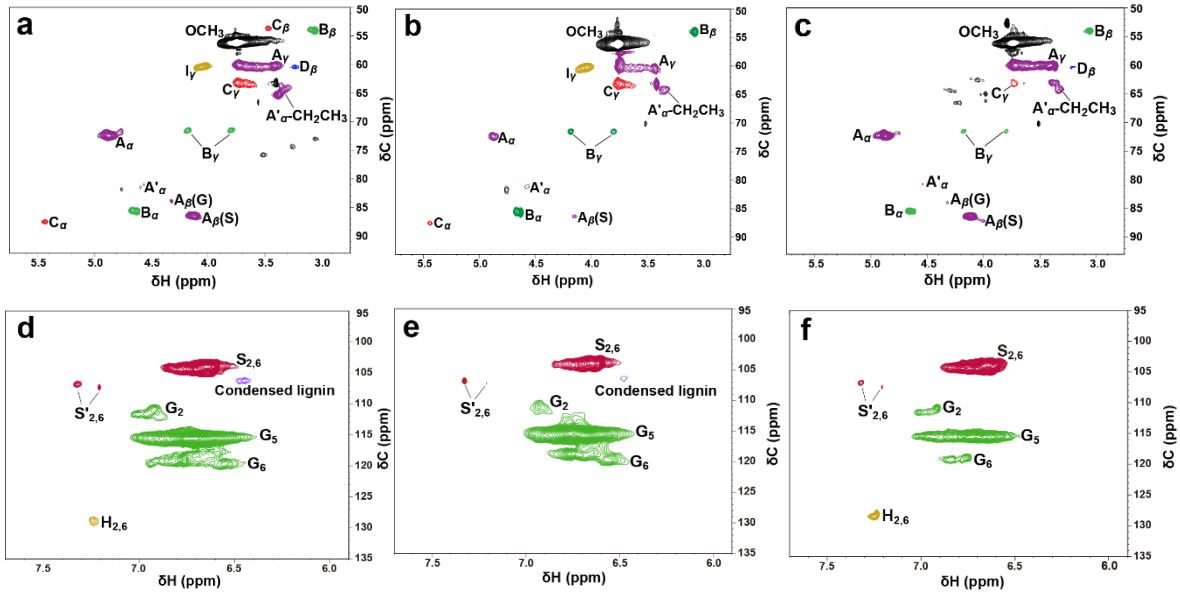

Fig. 4. The HSQC spectra of lignin fractions. The side chain region: AEOL (a), F2 (b), and F4 (c). The aromatic region: AEOL (d), F2 (e), and F4 (f)

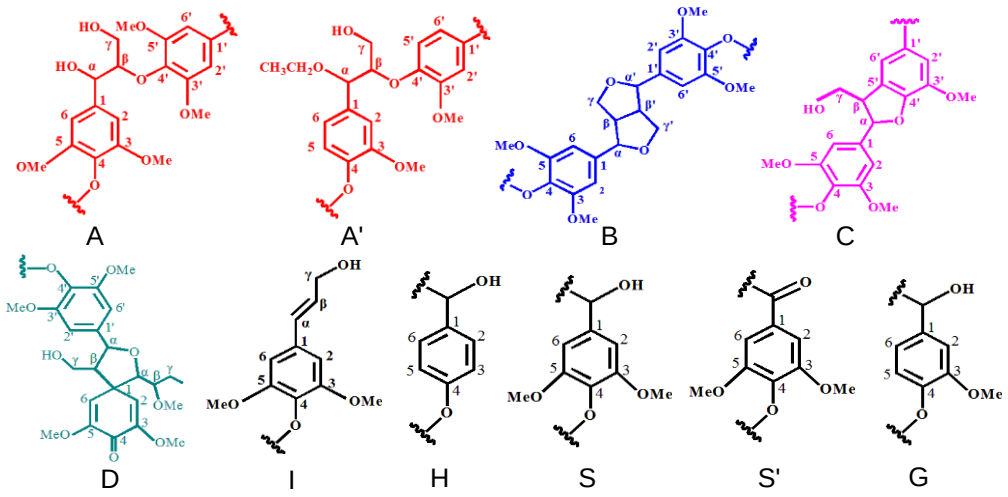

Fig. 5. Main lignin substructures in AEOL and fractionated lignins: (A) *β*-O-4' linkage; (A') C_α-ethoxylation-*β*-O-4' linkages; (B) resinol substructures formed by *β*-*β*' linkages; (C) phenylcoumaran substructures formed by *β*-5' linkages; (D) spirodienone substructure formed by *β*-1' linkages; (G) guaiacyl unit; (H) *p*-hydroxyphenyl unit; (I) cinnamyl alcohol end-groups; (S) syringyl unit; (S') oxidized syringyl units linked a carbonyl at C_α (phenolic)

After fractionation, the α-ethoxylated *β*-O-4' aryl ether substructures still remained in F2 and F4, implying that the lignins with such substructures were dispersed into the fractions during sequential extraction. Moreover, resinol substructures (B) were implied by the correlations at δ_C/δ_H 85.7/4.63 (B_α), 54.2/3.06 (B_β), and 71.6/3.80, 4.18 ppm (B_γ). Phenylcoumaran substructures (C) could be found with their signals at 87.6/5.51 (C_α), 53.8/3.47 (C_β), and 63.3/3.73 ppm (C_γ). Spirodienone structures (D) were identified based on the signals at δ_C/δ_H 81.87/4.76 (D_α) and 60.61/3.24 ppm (D_β).

In the aromatic region of HSQC spectra, the $C_{2,6}$-$H_{2,6}$ correlations of the S-units were found at δ_C/δ_H 104.5/6.70 ppm, while the weak correlations for the oxidized (*α*-ketone) structure (S') were identified at δ_C/δ_H 106.3/7.33 ppm. The cross-signals ascribed to G units were observed at δ_C/δ_H 111.2/6.92 (C_2-H_2), 115.7/6.75 (C_5-H_5), and 119.3/6.76 ppm (C_6-H_6), respectively. In addition, a small number of H units were observed with correlations at δ_C/δ_H 129.2/7.24 ppm. However, the signals of H units were not observed in F2, suggesting that the F2 fraction had fewer H-type lignin units, as revealed by the quantitative Py-GC/MS analysis. Finally, the C-H correlations from the condensed lignin structures in S units were founded at δ_C/δ_H 106.9/6.45 ppm in AEOL and F2, but not in the F4 fraction, indicating that condensed lignin was preferentially dissolved in ethyl acetate.

The relative content (referred to as a percentage of the total substructures) and the S/G ratios of the inter-unit linkages in the three lignin fractions were determined according to a previous publication (Qin *et al.* 2018a). As shown in Table 3, AEOL had a high proportion of *β*-O-4' linkages (66.5%) followed by *β*-*β*' linkages (18.8%). In addition, the proportions of *β*-5' (7.6%) and *β*-1' linkages (7.1%) were similar in AEOL. After fractionation, the *β*-*β*' and *β*-1' linkage proportions were increased greatly in F2, whereas *β*-5' linkage proportion was slightly enhanced compared to AEOL, indicating that the ethyl acetate fraction had more C-C linkages. In contrast, F4 showed a higher *β*-O-4' linkage proportion (69.6%) and a lower *β*-1' linkage proportion (3.9%). The S/G ratio of AEOL was 1.8. After fractionation, it was reduced to 1.4 in F2 and increased to 2.1 in F4. The relatively lower *β*-O-4' linkage proportion and lower S/G ratio in F2 indicated that the lignin fragments with a higher content of cleaved *β*-O-4' linkages of G-type lignin were selectively dissolved in ethyl acetate. The higher S/G ratio of F4 indicated that the lignin fragments with a higher S unit-rich lignin content were selectively dissolved in acetone. Additionally, the higher S/G ratio of F4 indicated that the acetone fraction had a more linear structure because the C5 position of the aromatic ring was not available for cross-linking (Crestini *et al*. 2011). In short, the lignin fractions collected after sequential extraction showed diverse structural features as compared with the original lignin.

Table 3. Quantification of the Lignin Fractions by 2D-HSQC NMR Spectra

Lignin Inter-unit Linkages	Percentage (%)		
	AEOL	F2	F4
β-O-4' Aryl ethers (A and A')	66.5	48.4	69.6
β-*β*' Resinols (B)	18.8	26.3	19.0
β-5' Phenylcoumarans (C)	7.6	9.6	7.4
β-1' Spirodienone (D)	7.1	15.7	3.9
S/G Ratio	1.8	1.4	2.1

^{31}P-NMR Spectra

To investigate the effects of sequential solvent fractionation on the number of hydroxyl groups, AEOL and its fractions were compared using ^{31}P NMR spectroscopy. The

amounts of aliphatic OH, carboxylic OH, syringyl phenolic OH, guaiacyl phenolic OH, and *p*-hydroxyphenyl phenolic OH were determined (Jiang *et al.* 2016; Jääskeläinen *et al.* 2017). The aliphatic OH in lignin was ascribed either to free OH in the side chain of the lignin molecules or to carbohydrates in the sample (Jääskeläinen *et al.* 2017). The aliphatic OH content in F5 was abundant compared to that of the other five lignin fractions (Table 4). This was because the greater content of carbohydrates in the F5 fraction elevated the aliphatic OH content. The content of carboxylic OH was nearly constant in all lignin fractions, meaning it was not affected by sequential solvent fractionation.

Table 4. Quantification of the Fractions by Quantitative ^{31}P-NMR Method (mmol/g)

Hydroxyl Groups	AEOL	F1	F2	F3	F4	F5
Aliphatic OH	1.6	1.3	1.2	1.6	1.4	2.0
Syringyl phenolic OH	0.8	1.0	1.1	0.8	0.7	0.7
Guaiacyl phenolic OH	1.4	0.5	1.4	1.2	1.0	0.9
p-Hydroxyphenyl phenolic OH	0.3	0.1	0.3	0.4	0.2	0.1
Carboxylic OH (COOH)	0.3	0.2	0.3	0.2	0.3	0.4
Total phenolic OH	2.5	1.6	2.8	2.4	1.9	1.7

The total phenolic OH content of F2, F3, F4, and F5 fractions decreased as the molecular weight increased, which was consistent with the results of earlier reports (Li *et al.* 2012; Jiang *et al.* 2016). Generally, the cleavage of *β*-O-4' linkages of lignin macromolecule led to higher phenolic content in lignin fractions. In other words, the phenolic OH content of lignin showed a negative correlation to the molecular weight (Sadeghifar *et al.* 2017). Although the F1 fraction had the lowest molecular weight, it also had the least amount of total phenolic OH (1.6 mmol/g). This result could be explained by the presence of extractives in the F1 fraction. In contrast, the F2 fraction exhibited the highest total phenolic OH content (2.8 mmol/g). This higher content in F2 suggested that F2 contained more AEOL fragments with low molecular weight, *i.e.*, the cleavage of *β*-O-4′ linkages led to more phenolic OH (Pan *et al.* 2006). This was consistent with the result that F2 showed the lowest *β*-O-4' linkages proportion (Table 3) and the lowest molecular weight except for F1 (Table 1). For the industrial application of natural antioxidants, the most important functional groups in lignin's chemical structure are hydroxyl groups linked to the benzene ring, *i.e.*, phenolic OH, because they are most powerful in capturing and neutralizing free radicals (Li *et al.* 2012; Michelin *et al.* 2018). The highest total phenolic OH content in F2 indicates that it had the greatest potential for use as a natural antioxidant in industrial products, *e.g.*, pharmaceuticals and cosmetics.

Antioxidant Performance

DPPH radical scavenging activity

The antioxidant activity of AEOL and its fractions were compared to BHT, a synthetic antioxidant that is commonly used both in commercial products and as a control in antioxidant studies. Figure 6(a) depicts the DPPH scavenging curves of the lignin fractions, and Fig. 6(b) shows corresponding radical-scavenging index (RSI) values. The results show that AEOL had higher RSI values compared to BHT. After fractionation, a remarkable increase in RSI values were observed for F2 and F3 in relation to AEOL, while a serious decrease in RSI values was observed for F1 and F5 in comparison to AEOL. Notably, the scavenging activities of the lignin fractions showed a negative correlation with

molecular weight, whereas a positive correlation was found between AEOL antioxidant activities and the total phenolic OH content. Generally, the antioxidant property of lignin was related to the capability of phenolic OH to capture and neutralize the DPPH radical, *i.e.*, lignin with higher phenolic OH content had higher antioxidant property (An *et al.* 2017; Michelin *et al.* 2018). In contrast, antioxidant activity decreased in the presence of carbohydrates, *α*-carbonyl groups, and aliphatic OH groups (Dizhbite *et al.* 2004; Qin *et al.* 2018a). The high antioxidant activity of F2 (RSI = 15.1) could be attributed to its low molecular weight, narrow polydispersity, and high phenolic OH content. The lower RSI values of F1 (RSI = 5.5) resulted from the fact that the fraction contained extractives. However, the low phenolic OH content, high aliphatic OH content, and high molecular weight of F5 led to a lower RSI (RSI = 6.3) value. Lignin fractions with low molecular weight, such as F1 and F2, probably contained a small number of lower-mass phenolic compounds. These phenolic compounds showed positive effect on the antioxidant activities of these fractions. But the lignin component still played a key functional role in the antioxidant activities according to result of DPPH assay.

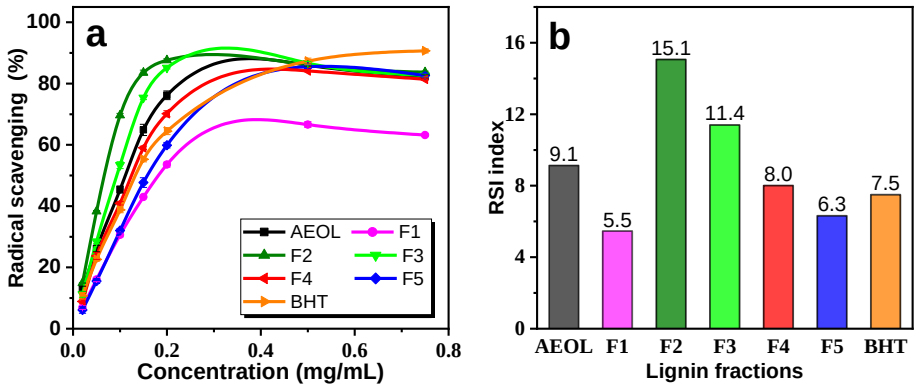

Fig. 6. Antioxidant activity against DPPH of AEOL, five lignin fractions, and BHT; (a) DPPH free radical scavenging capacity; (b) RSI value

Reducing power

The reducing power is a noticeable indicator of whether a substance is a promising antioxidant. The reducing capacity of compounds is related to the strength of its electron donating activity, which is general polyphenolic polymer antioxidant activity (An *et al.* 2017). In the present study, the reducing capacity of different concentrations of AEOL and five fractions were assessed and compared with the control antioxidant reagent (*i.e.*, BHT). The results are displayed in Fig. 7. The absorbance of all fractions and BHT presented a steady increase with increasing concentrations. The reducing capacity of AEOL was higher than BHT in the concentrations ranging from 0.05 to 0.15 mg/mL, whereas the lower reducing capacity of AEOL was observed at concentrations higher than 0.2 mg/mL. Remarkably, F1, F2, and F3 fractions always exhibited a higher reducing capacity than BHT, indicating that fractionation increased the reducing capacity. As stated, F2 exhibited the highest reducing power among all lignin fractions. This result is consistent with its ability to scavenge DPPH radicals, and both results likely can be attributed to the highest phenolic OH content in F2. In general, the reducing capacities of F2, F3, F4, and F5 decreased as the molecular weight increased at all the tested concentrations, illustrating that molecular weight was additionally an important parameter that affected the reducing capacity of AEOL.

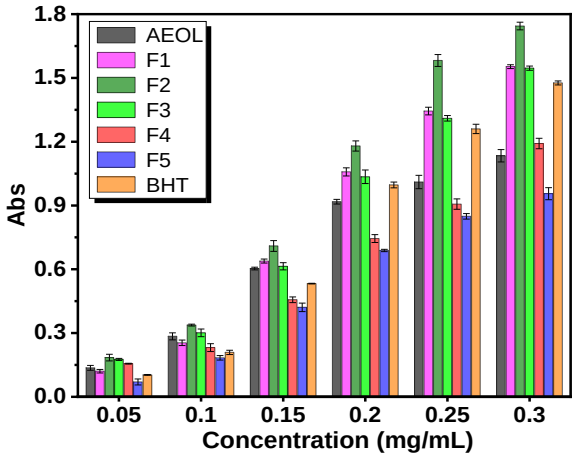

Fig. 7. Reducing power of AEOL, five lignin fractions, and BHT

CONCLUSIONS

1. This study indicated that lignin material with a homogeneous structure and enhanced antioxidant performance can be obtained by sequential solvent fractionation process. In addition, it demonstrated that Chinese quince fruits are a potentially valuable natural resource.
2. Sugar analysis of the lignin fractions highlighted a decrease of sugar content upon fractionation; the carbohydrate mainly existed in the high molecular weight fraction (dioxane/water fraction).
3. The fractionation yields were observed to be highest for methanol (43.8%), followed by dioxane/water (18.6%), and ethyl acetate (13.5%).
4. The obtained five lignin fractions (F1 through F5) showed increasing molecular weight in the range of 600 to 12000 g/mol. The ethyl acetate fraction with M_w of 1082 g/mol showed a low proportion of β-O-4' linkages (48.4%) and the highest phenolic OH content of 2.8 mmol/g.
5. As the molecular weight increased, the phenolic OH content of the lignin fractions decreased from F2 to F5.
6. The antioxidant activity assays show that the ethyl acetate fraction has remarkable DPPH scavenging activity and reducing power.

ACKNOWLEDGMENTS

The authors are grateful for the support of the Technological Innovation Talents of Colleges and Universities (19HASTIT012), the National Natural Science Foundation of China (U1804111) and the Earmarked Fund for Modern Agro-industry Technology Research System (CARS14-1-29).

REFERENCES CITED

An, L., Wang, G., Jia, H., Liu, C., Sui, W., and Si, C. (2017). "Fractionation of enzymatic hydrolysis lignin by sequential extraction for enhancing antioxidant performance," *Int. J. Biol. Macromol.* 99, 674-681. DOI: 10.1016/j.ijbiomac.2017.03.015

Arshanitsa, A., Ponomarenko, J., Dizhbite, T., Andersone, A., Gosselink, R. J. A., van der Putten, J., Lauberts, M., and Telysheva, G. (2013). "Fractionation of technical lignins as a tool for improvement of their antioxidant properties," *J. Anal. Appl. Pyrol.* 103, 78-85. DOI: 10.1016/j.jaap.2012.12.023

Catignani, G. L., and Carter, M. E. (1982). "Antioxidant properties of lignin," *J. Food Sci.* 47(5), 1745-1745. DOI: 10.1111/j.1365-2621.1982.tb05029.x

Cheng, X.-C., Guo, X.-R., Qin, Z., Wang, X.-D., Liu, H.-M., and Liu, Y.-L. (2020). "Structural features and antioxidant activities of Chinese quince (*Chaenomeles sinensis*) fruit lignin during auto-catalyzed ethanol organosolv pretreatment," *Int. J. Biol. Macromol.* 164, 4348-4358. DOI: 10.1016/j.ijbiomac.2020.08.249

Costa, C. A. E., Pinto, P. C. R., and Rodrigues, A. E. (2018). "Lignin fractionation from *E. Globulus* kraft liquor by ultrafiltration in a three stage membrane sequence," *Sep. Purif. Technol.* 192, 140-151. DOI: 10.1016/j.seppur.2017.09.066

Crestini, C., Melone, F., Sette, M., and Saladino, R. (2011). "Milled wood lignin: A linear oligomer," *Biomacromolecules* 12, 3928-3935. DOI: 10.1021/bm200948r

del Río, J. C., Prinsen, P., Rencoret, J., Nieto, L., Jiménez-Barbero, J., Ralph, J., Martínez, Á. T., and Gutiérrez, A. (2012). "Structural characterization of the lignin in the cortex and pith of elephant grass (*Pennisetum purpureum*) stems," *J. Agr. Food Chem.* 60, 3619-3634. DOI: 10.1021/jf300099g

Dizhbite, T., Telysheva, G., Jurkjane, V., and Viesturs, U. (2004). "Characterization of the radical scavenging activity of lignins−natural antioxidants," *Bioresource Technol.* 95(3), 309-317. DOI: 10.1016/j.biortech.2004.02.024

dos Santos, P. S. B., Erdocia, X., Gatto, D. A., and Labidi, J. (2014). "Characterisation of kraft lignin separated by gradient acid precipitation," *Ind. Crop. Prod.* 55, 149-154. DOI: 10.1016/j.indcrop.2014.01.023

Hamauzu, Y., Takedachi, N., Miyasaka, R., and Makabe, H. (2010). "Heat treatment of Chinese quince polyphenols increases rat plasma levels of protocatechuic and vanillic acids," *Food Chem.* 118(3), 757-763. DOI: 10.1016/j.foodchem.2009.05.054

Huang, Y., Lai, C., Sun, S., Yong, Q., Via, B. K., and Tu, M. (2020). "Organosolv lignin properties and their effects on enzymatic hydrolysis," *BioResources* 15(4), 8909-8924. DOI: 10.15376/biores.15.4.8909-8924

Inkrod, C., Raita, M., Champreda, V., and Laosiripojana, N. (2018). "Characteristics of lignin extracted from different lignocellulosic materials *via* organosolv fractionation," *Bioenerg. Res.* 11, 277-290. DOI: 10.1007/s12155-018-9895-2

Jääskeläinen, A.-S., Liitiä, T., Mikkelson, A., and Tamminen, T. (2017). "Aqueous organic solvent fractionation as means to improve lignin homogeneity and purity," *Ind. Crop. Prod.* 103, 51-58. DOI: 10.1016/j.indcrop.2017.03.039

Jiang, X., Savithri, D., Du, X., Pawar, S., Jameel, H., Chang, H.-M., and Zhou, X. (2016). "Fractionation and characterization of kraft lignin by sequential precipitation with various organic solvents," *ACS Sustain. Chem. Eng.* 5, 835-842. DOI: 10.1021/acssuschemeng.6b02174

Kim, J.-Y., Johnston, P. A., Lee, J. H., Smith, R. G., and Brown, R. C. (2019). "Improving lignin homogeneity and functionality *via* ethanolysis for production of

antioxidants," *ACS Sustain. Chem. Eng.* 7(3), 3520-3526. DOI: 10.1021/acssuschemeng.8b05769

Kirk, T. K., Brown, W., and Cowling, E. B. (1969). "Preparative fractionation of lignin by gel-permeation chromatography," *Biopolymers* 7(2), 135-153. DOI: 10.1002/bip.1969.360070202

Lange, H., Schiffels, P., Sette, M., Sevastyanova, O., and Crestini, C. (2016). "Fractional precipitation of wheat straw organosolv lignin: Macroscopic properties and structural insights," *ACS Sustain. Chem. Eng.* 4(10), 5136-5151. DOI: 10.1021/acssuschemeng.6b01475

Li, M.-F., Sun, S.-N., Xu, F., and Sun, R.-C. (2012). "Sequential solvent fractionation of heterogeneous bamboo organosolv lignin for value-added application," *Sep. Purif. Technol.* 101, 18-25. DOI: 10.1016/j.seppur.2012.09.013

Michelin, M., Liebentritt, S., Vicente, A. A., and Teixeira, J. A. (2018). "Lignin from an integrated process consisting of liquid hot water and ethanol organosolv: Physicochemical and antioxidant properties," *Int. J. Biol. Macromol.* 120(Part A), 159-169. DOI: 10.1016/j.ijbiomac.2018.08.046

Pan, X., Kadla, J. F., Ehara, K., Gilkes, N., and Saddler, J. N. (2006). "Organosolv ethanol lignin from hybrid poplar as a radical scavenger: Relationship between lignin structure, extraction conditions, and antioxidant activity," *J. Agr. Food Chem.* 54(16), 5806-5813. DOI: 10.1021/jf0605392

Passoni, V., Scarica, C., Levi, M., Turri, S., and Griffini, G. (2016). "Fractionation of industrial softwood kraft lignin: Solvent selection as a tool for tailored material properties," *ACS Sustain. Chem. Eng.* 4(4), 2232-2242. DOI: 10.1021/acssuschemeng.5b01722

Qin, Z., Zhang, Z.-G., Liu, H.-M., Qin, G.-Y., and Wang, X.-D. (2018a). "Acetic acid lignins from Chinese quince fruit (*Chaenomeles sinensis*): Effect of pretreatment on their structural features and antioxidant activities," *RSC Adv.* 8(44), 24923-24931. DOI: 10.1039/C8RA04009E

Qin, Z., Ma, Y.-X., Liu, H.-M., Qin, G.-Y., and Wang, X.-D. (2018b). "Structural elucidation of lignin-carbohydrate complexes (LCCs) from Chinese quince (*Chaenomeles sinensis*) fruit," *Int. J. Biol. Macromol.* 116, 1240-1249. DOI: 10.1016/j.ijbiomac.2018.05.117

Qin, Z., Wang, X.-D., Liu, H.-M., Wang, D.-Y., and Qin, G.-Y. (2018c). "Structural characterization of Chinese quince fruit lignin pretreated with enzymatic hydrolysis," *Bioresource Technol.* 262, 212-220. DOI: 10.1016/j.biortech.2018.04.072

Sadeghifar, H., Wells, T., Le, R. K., Sadeghifar, F., Yuan, J. S., and Ragauskas, A. J. (2017). "Fractionation of organosolv lignin using acetone: Water and properties of the obtained fractions," *ACS Sustain. Chem. Eng.* 5(1), 580-587. DOI: 10.1021/acssuschemeng.6b01955

Smink, D., Kersten, S. R. A., and Schuur, B. (2020). "Comparing multistage liquid-liquid extraction with cold water precipitation for improvement of lignin recovery from deep eutectic solvents," *Sep. Purif. Technol.* 252, Article ID 117395. DOI: 10.1016/j.seppur.2020.117395

Song, Y., Shi, X., Yang, X., Zhang, X., and Tan, T. (2020). "Successive organic solvent fractionation and characterization of heterogeneous lignin extracted by *p*-toluenesulfonic acid from hybrid poplar," *Energ. Fuel.* 34, 557-567. DOI: 10.1021/acs.energyfuels.9b03508

Ugartondo, V., Mitjans, M., and Vinardell, M. P. (2008). "Comparative antioxidant and cytotoxic effects of lignins from different sources," *Bioresource Technol.* 99(14), 6683-6687. DOI: 10.1016/j.biortech.2007.11.038

Vinardell, M. P., Ugartondo, V., and Mitjans, M. (2008). "Potential applications of antioxidant lignins from different sources," *Ind. Crop. Prod.* 27(2), 220-223. DOI: 10.1016/j.indcrop.2007.07.011

Wen, J.-L., Sun, S.-L., Xue, B.-L., and Sun, R.-C. (2013). "Quantitative structures and thermal properties of birch lignins after ionic liquid pretreatment," *J. Agr. Food Chem.* 61(3), 635-645. DOI: 10.1021/jf3051939

Wen, J.-L., Sun, S.-L., Xue, B.-L., and Sun, R.-C. (2015). "Structural elucidation of inhomogeneous lignins from bamboo," *Int. J. Biol. Macromol.* 77, 250-259. DOI: 10.1016/j.ijbiomac.2015.03.044

Yang, H., Yan, J., and Li, J. (2020). "Preliminary study on integrated production of ethanol and lignin from bagasse pulp waste," *BioResources* 15(4), 8161-8174. DOI: 10.15376/biores.15.4.8161-8174

Zhou, S., Xue, Y., Sharma, A., and Bai X. (2016). "Lignin valorization through thermochemical conversion: comparison of hardwood, softwood and herbaceous lignin," *ACS Sustain. Chem. Eng.* 4(12), 6608-6617. DOI: 10.1021/acssuschemeng.6b01488

Article submitted: December 30, 2020; Peer review completed: February 7, 2021; Revised version received and accepted: February 18, 2021; Published: February 22, 2021.
DOI: 10.15376/biores.16.2.2714-2730